Mechanism of CO Oxidation by Carbon Monoxide Dehydrogenase from *Clostridium thermoaceticum* and Its Inhibition by Anions†

Javier Seravalli, Manoj Kumar, Wei-Ping Lu, and Stephen W. Ragsdale*

Department of Biochemistry, East Campus, University of Nebraska, Lincoln, Nebraska 68583-0718

Received January 4, 1995; Revised Manuscript Received March 27, 1995®

ABSTRACT: Carbon monoxide dehydrogenase (CODH) performs two distinct reactions at two different metal centers. The synthesis of acetyl-CoA from a methyl group, CO, and coenzyme A occurs at center A and the oxidation of CO to CO_2 occurs at center C. In the work reported here, we have studied the mechanism of CO oxidation by CODH and its inhibition by thiocyanate. Our data are consistent with a ping-pong mechanism. A scheme to explain the first half-reaction was developed that includes binding of water and CO to the oxidized form of center C, deprotonation of coordinated water to yield enzyme-bound hydroxyl, nucleophilic attack on coordinated CO by OH^- to form enzyme-bound carboxyl, and deprotonation and decarboxylation to form CO_2 and the reduced form of center C. In the second half-reaction, the reduced enzyme is reoxidized by an electron acceptor. CO oxidation was pH dependent. The pH dependence of k_{cat}/K_m for CO gave a single pK_a of 7.7 and a maximum value at 55 °C and high pH of 9.1×10^6 M^{-1} s^{-1}. The pH dependence of k_{cat} followed a two-phase titration curve with pK_a values of 7.1 and 9.5 and maximum value of k_{cat} at 55 °C and high pH of 3250 s^{-1} (1310 μmol of CO oxidized min^{-1} mg^{-1}). The pH dependencies of k_{cat}/K_m and k_{cat} are interpreted to reflect the ionization of enzyme-bound water from binary and ternary complexes with center C. Reaction with thiocyanate, azide, or cyanate was found to cause a striking shift in the EPR spectrum of center C from $g_{av} = 1.82$ ($g = 2.01, 1.81, 1.65$) to a two-component spectrum with $g_{av} = 2.15$ ($g = 2.34, 2.067, 2.03$) and $g_{av} = 2.17$ ($g = 2.34, 2.115, 2.047$). Thiocyanate acted as a mixed partial inhibitor with respect to CO. The inhibition constants were pH and temperature dependent. The pH dependencies of the inhibition constants gave pK_a values of ~7.7. Binding of thiocyanate to the oxidized form of center C appears to be favored by a negative enthalpy that is offset by a decrease in entropy yielding a slightly unfavorable free energy of association.

The reductive acetyl-CoA pathway, also called the Wood pathway or the Wood–Ljungdahl pathway, plays an important role in the global carbon cycle. It allows sulfate reducers, methanogens, and acetogens to convert CO or CO_2 to cell carbon (Fuchs, 1986; Ljungdahl, 1986; Ragsdale, 1991). Key enzymes operate in reverse in some methanogens to convert acetic acid to methane (Thauer *et al.*, 1989; Ferry, 1992a,b). Unique aspects of the acetyl-CoA pathway include a preponderance of enzyme-bound intermediates, the involvement of metal–carbon bonds, and a strategy of carbon–carbon bond formation that is similar to some well-studied organometallic reactions in solution (Ragsdale, 1994).

An important reaction in the acetyl-CoA pathway is the reversible oxidation of CO to CO_2. When the bacteria grow on CO, they must oxidize CO to CO_2 since the methyl group of acetyl-CoA derives from CO_2. Since the carbonyl group of acetyl-CoA derives from CO, reduction of CO_2 to CO is required when bacteria are grown on hydrogen and CO_2 or on organic substrates, such as sugars or aromatic compounds. The enzyme that catalyzes CO oxidation and CO_2 reduction is carbon monoxide dehydrogenase (CODH). The enzymatic oxidation of CO is analogous to the water–gas shift reaction, which is an important industrial process that is catalyzed by inorganic complexes. A Ni(II) complex has been described that acts as a functional model of CO oxidation (Lu *et al.*, 1993). The catalytic reduction of CO_2 to CO has been described in several Ni model systems (Begley *et al.*, 1986; Aresta *et al.*, 1988).

CODH is one of the few nickel proteins in nature, containing 2 Ni, 9–13 Fe, ~1 Zn, and 14 S^{2-} per 150 kDa dimer (Ragsdale *et al.*, 1983a). Three distinct metal centers have been characterized (Ragsdale *et al.*, 1982, 1983b, 1985; Lindahl *et al.*, 1990a,b; Fan *et al.*, 1991; Shin *et al.*, 1992), that are now called centers A, B, and C. There is another species, "ferrous component II", that was detected by Mössbauer spectroscopy (Lindahl *et al.*, 1990b) and is either separate or a component of one of the other centers.

Recent studies show that CODH has two active sites, centers A and C. Center A is the site of acetyl-CoA synthesis (Gorst & Ragsdale, 1991; Shin & Lindahl, 1992; Kumar *et al.*, 1993), and center C is the site for CO oxidation (Anderson *et al.*, 1993b; Kumar *et al.*, 1993). CO binds to center A to elicit an EPR signal (Ragsdale *et al.*, 1982) that has been called the Ni–Fe–C signal and originates from the adduct between CO and a cluster containing Ni and Fe (Ragsdale *et al.*, 1985). CO was shown to bind end-on to an iron component of this mixed-metal cluster to give [Ni–X–Fe_3–4–S_4]–C≡O (Kumar & Ragsdale, 1992; Qiu *et al.*, 1994, 1995). The center A–CO adduct has been shown to be catalytically competent in acetyl-CoA synthesis (Gorst

† This paper has been assigned Journal Series No. 10996, Agricultural Research Division, University of Nebraska. This work was supported by grants to S.W.R. from the National Institutes of Health (GM 39451) and the Department of Energy (ER 20053).

* Corresponding author. Phone: 402-472-2943. Facsimile: 402-472-7842. Internet: sragsdale@crcvms.unl.edu.

® Abstract published in *Advance ACS Abstracts,* June 1, 1995.

0006-2960/95/0434-7879$09.00/0

& Ragsdale, 1991; Kumar *et al.*, 1993) but *not* kinetically competent in CO oxidation (Kumar *et al.*, 1993).

In this paper, we have focused on the catalytic mechanism of CO oxidation, which is not well understood. Freeze-quench EPR studies were instrumental in identifying center C as the site of CO oxidation (Kumar *et al.*, 1993). Binding of CO to center C occurs with a rate constant of $\sim 2 \times 10^8$ M^{-1} s^{-1} at 55 °C. This is ~10-fold faster than the k_{cat}/K_m for CO oxidation, demonstrating the kinetic competence of the center C−CO adduct. Cyanide was shown to specifically inhibit CO oxidation with little effect on acetyl-CoA synthesis (Ragsdale *et al.*, 1983a; Ragsdale & Wood, 1985; Raybuck *et al.*, 1988). In the work described here, we have characterized another inhibitor of CO oxidation, thiocyanate, and developed a scheme to describe its mode of interaction with center C of CODH.

Although the structure of center C is not known, spectroscopic studies have given insight into its nature. The EPR spectra of a center in the CODHs of *Rhodospirillum rubrum* (Bonam & Ludden, 1987; Stephens *et al.*, 1989) and *Clostridium thermoaceticum* (Ragsdale *et al.*, 1982; Lindahl *et al.*, 1990a) are highly similar indicating that center C is present in both CODHs. In contrast, center A and acetyl-CoA synthesis activity are absent from the *R. rubrum* enzyme. Center C of the *R. rubrum* enzyme was proposed to contain nickel because there is ~8 G broadening of the low-field feature of the EPR spectrum of the ^{61}Ni-substituted enzyme (Stephens *et al.*, 1989). Evidence that nickel is a component of center C in the CODH from *C. thermoaceticum* has been provided by freeze-quench resonance Raman spectroscopy of the CO adduct with CODH (Qiu *et al.*, 1995). Significant ^{57}Fe hyperfine broadening has been observed for the CODHs from both *R. rubrum* (Stephens *et al.*, 1989) and *C. thermoaceticum* (Lindahl *et al.*, 1990a). Therefore, like center A (Ragsdale *et al.*, 1985), center C appears to be a Ni/Fe-S cluster. Ni EXAFS of the *R. rubrum* enzyme indicate that nickel is not part of a cubane center (Tan *et al.*, 1992); thus, Ni and Fe must be bridged by a common external ligand.

The inhibitor cyanide has been shown to bind to center C of *C. thermoaceticum* by EPR and ENDOR spectroscopies (Anderson *et al.*, 1993a). It also was proposed to bind to a nickel site in center C in the *R. rubrum* CODH (Ensign *et al.*, 1989a,b). In the work reported here, we demonstrated that thiocyanate also binds to center C and elicits large changes in the EPR spectrum of center C.

MATERIALS AND METHODS

Materials. CO (99.9%) and N_2 (99.998%) were obtained from Linweld, Lincoln, NE. N_2 and other inert gases were purified of oxygen by passage through a column of heated BASF catalyst. Sodium thiocyanate and sodium azide were of Ultra pure grade from Aldrich. [^{15}N]Azide was obtained from Cambridge Isotope Labs and ^{61}Ni from Advance Materials and Technology (New York). All other chemicals were of highest available purity and were used as supplied.

Growth of Organism and Enzyme Purification. C. thermoaceticum strain ATCC 39073 was grown on glucose as a carbon source at 55 °C as previously described (Andreesen *et al.*, 1973). Purification of CODH was done under strictly anaerobic conditions essentially as described (Ragsdale *et al.*, 1983a) except that the ammonium sulfate precipitation step was omitted. The procedure was performed in an anaerobic chamber (Vacuum Atmospheres, Hawthorne, CA) maintained at 17 °C and below 1 ppm oxygen. The enzyme was stored in liquid nitrogen. The average specific activity of the purified CODH was 430 units/mg (1 unit = 1 μmol of CO oxidized/min) at 55 °C in the standard assay performed at pH 7.6 with 10 mM methyl viologen as electron acceptor (Ragsdale *et al.*, 1983a). Protein concentrations were determined by a dye-binding assay using Rose Bengal (Elliott & Brewer, 1978).

Kinetics of CO Oxidation and CO_2 Reduction. CO oxidation was followed at 25 °C by monitoring the formation of reduced methyl viologen according to eq 1a or 1b where

$$CO + H_2O + 2MV_{OX} \rightleftharpoons CO_2 + 2H^+ + 2MV_{red} \quad (1a)$$

$$CO + HO^- + 2MV_{OX} \rightleftharpoons CO_2 + H^+ + 2MV_{red} \quad (1b)$$

MV_{ox} and MV_{red} are oxidized and reduced methyl viologen, respectively. Earlier experiments indicated that water, not hydroxide, is the substrate and CO_2, not bicarbonate, is the product of this reaction (Bott & Thauer, 1989) as shown by eq 1a.

The assay mixture contained a saturated solution of CO (900 μM) (Budavari, 1989) and 10 mM methyl viologen. The complete time course was followed at 504 nm [the molar extinction coefficient (ϵ) was determined to be 6575 M^{-1} cm^{-1}] using glass cuvettes with a 2 mm path length. The total absorbance change was between 2.0 and 2.5. An OLIS updated Cary-14 spectrophotometer controlled by an IBM-PC computer, and OLIS software was used for data acquisition. Temperature was maintained at 25 °C by a NESLAB water circulation bath. Typical assays were prepared in a 650 μL cuvette by mixing buffer and thiocyanate solutions to a volume of 540 μL. After slowly bubbling with CO at room temperature for 5−10 min, 1−5 μL of CODH stock solution (10−20 μM) was added followed by 60 μL of 100 mM MV to start the reaction. The pH dependencies of the kinetic parameters were measured in reactions containing MES buffers from pH 6.5 to 7.0, Tris-HCl buffers from pH 7.0 to 9.5, and CAPSO buffers above pH 9.5. The pH was measured at the end of most assays using a Corning Model 240 pH meter calibrated at pH 4.0, pH 7.0, and pH 10.0 with standard buffers (Fisher).

To study the mode of thiocyanate inhibition with respect to CO, V_{max} and V_{max}/K_m for CO were determined using the integrated Michaelis−Menten eq 2, where A_o, A_i, and A are

$$A = A_i - (A_i - A_Q) \exp\left\{(V_{max}/K_m)\left(\frac{(A - A_o)}{V_{max}} - t\right)\right\} \quad (2)$$

the absorbances at initial time, final time, and time "t", respectively.

After subtracting A from both sides so that all variables are on the right side, values of A_o, A_i, V_{max}/K_m in min^{-1}, and V_{max} in OD min^{-1} were obtained by fitting the resulting equation to zero by nonlinear regression using the program Sigma-Plot.[1] Use of the integrated Michaelis−Menten equation is valid only under certain conditions (Segel, 1975). We obtained the same values of V_{max} and V_{max}/K_m by initial velocity experiments at pH 7.60 (below) and by use of the integrated equation, demonstrating that this treatment was

valid. Unless otherwise stated, all kinetic parameters refer to the values measured at 25 °C. The values of V_{max}/K_m and V_{max} were then divided by the concentration of $\alpha\beta$ CODH dimers using a molecular mass of 149 kDa. The pH dependence of k_{cat}/K_m was determined by fitting the data to eq 3 to give K_{as}. Similarly, the pH dependence of k_{cat} was determined from a fit to eq 4 to yield values of K_{ai1} and K_{ai2}.

$$\log\{k_{cat}/K_m\} = \log\left\{(k_{cat}/K_m)_{max}\left(\frac{K_{as}}{K_{as} + 10^{-pH}}\right)\right\} \quad (3)$$

$$\log(k_{cat}) = \log\left\{k_{cat_1}\frac{K_{ai1}}{K_{ai1} + 10^{-pH}} + k_{cat_2}\frac{K_{ai2}}{K_{ai2} + 10^{-pH}}\right\} \quad (4)$$

Inhibition by thiocyanate of the reduction of CO_2 was studied at pH 6.00 by the initial rate method using 2 mM sodium dithionite and 4.0 μM horse hemoglobin in 150 mM MES buffer as previously described (Kumar *et al.*, 1994). The dependence of the apparent k_{cat}/K_m on the concentration of thiocyanate was determined by fitting the data to eq 5 to

$$V_{max}/K_m = (V_{max}/K_m)_0\frac{K_{is}}{K_{is} + [NaSCN]} + (V_{max}/K_m)_{in} \quad (5)$$

$$V_{max} = (V_{max})_0\frac{K_{ii}}{K_{ii} + [NaSCN]} + (V_{max})_{in} \quad (6)$$

yield a value for K_{is}. A similar replot of the apparent k_{cat} versus thiocyanate concentration yielded a value for K_{ii} according to eq 6. The values of $(V_{max}/K_m)_o$, $(V_{max})_o$, $(V_{max}/K_m)_{in}$, and $(V_{max})_{in}$ are V_{max}/K_m and V_{max} in the absence of thiocyanate and at saturating thiocyanate (fully inhibited enzyme), respectively.

EPR Spectroscopy. EPR spectra were recorded on a Bruker ESP 300E spectrometer equipped with an Oxford ITC4 temperature controller, automatic frequency counter (Hewlett Packard, Model 5340A), and gauss meter (Bruker). Spin concentrations were measured by comparing the double integrals (using supplied Bruker software) of the spectra with those of a 1 mM copper perchlorate standard. Spectroscopic parameters are stated in the figure legends. EPR spectra were simulated using the program XPOW (Belford & Nilges, 1979; Nilges, 1979; Altman, 1981; Maurice, 1982; Duliba, 1983) and graphed by Sigma-Plot (Jandel Scientific). To determine the saturation behavior of the EPR signals, the response of the EPR signal to increased microwave power was evaluated. The value of $P_{1/2}$, the power for half-saturation with microwave energy, was obtained from simulation of experimental data points with an empirical formula (eq 7) (Rupp *et al.*, 1978), where S represents the

$$S \propto \frac{P^{0.5}}{[1 + (P/P_{1/2})]^{0.5b}} \quad (7)$$

signal amplitude, P refers to the microwave power, and b is a variable that ranges from 1.0 (inhomogeneous broadening) to 2.0 (homogeneous broadening).

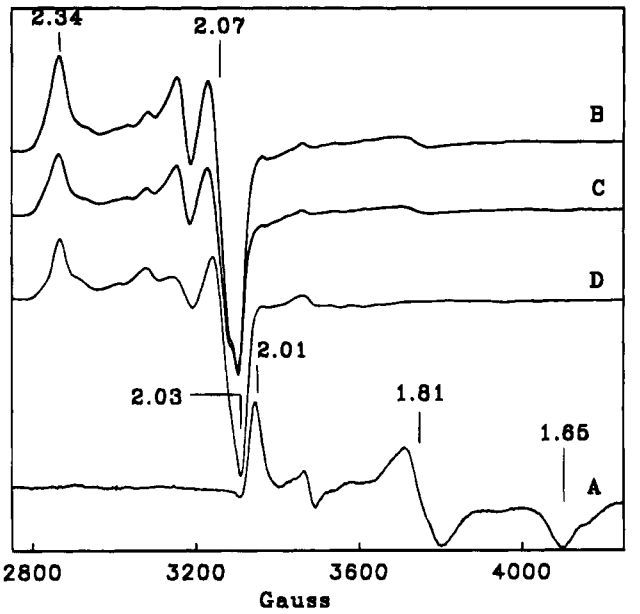

FIGURE 1: EPR spectra of the thiocyanate adduct with CODH. (A) Natural abundance CODH (50 μM, final) in 2 mM DTT and 50 mM Tris-HCl, pH 7.6. EPR parameters: temperature, 10 K; microwave power, 40 mW; microwave frequency, 9.4414 GHz; gain, 2×10^4; modulation amplitude, 10 G; modulation frequency, 100 kHz. (B) Natural abundance CODH (50 μM, final) treated with 10 mM sodium thiocyanate at 14 °C for 10 min before freezing and storing in liquid nitrogen. (C) ^{61}Ni-substituted CODH sample treated with 10 mM thiocyanate. (D) ^{57}Fe-substituted CODH sample treated with 10 mM thiocyanate. The hyperfine broadening is ~6 G.

RESULTS

Spectroscopic Studies of Center C of CODH and Its Reaction with Anions. When CODH samples were free of reductants, such as sodium dithionite, the only EPR spectrum observed was from center C, with g values at 2.01, 1.81, and 1.65 ($g_{av} = 1.82$) (Figure 1A). The $g \sim 2.01$ resonance has the narrowest line width and, thus, can be easily defined without having to simulate the spectra. The observed g value of this resonance was plotted versus pH and fit to

$$g = g_H + \delta g[10^{-pK_a}/(10^{-pk_a} + 10^{-pH})] \quad (8)$$

where g is the measured g value, g_H is the calculated limiting g value at low pH, and δg is difference between g_H and the limiting g value at high pH. The pK_a value for the transition was 7.2 ± 0.1 (Figure 2). The g values for the other two resonances from center C were treated similarly to obtain the following g values for the protonated and unprotonated forms of center C: 2.005, 1.815, 1.651 (low pH) and 2.015, 1.800, 1.638 (high pH).

Upon reaction of CODH in the state just described with thiocyanate, a marked change in the EPR spectrum was observed in which all the g values were above 2.0 (Figure 1B). Although we have recently demonstrated that both Ni

[1] Subtraction of the term A is required to perform a nonlinear regression fit to eq 2. The usual method of regression is to fit time versus absorbance in the form

$$t = \frac{A - A_o}{\epsilon V_{max}} + \frac{K_m}{V_{max}}\ln\frac{(A_i - A_o)}{A_i - A}$$

This method is cumbersome, particularly when one wishes to compare the goodness of a integrated Michaelis–Menten fit versus a first-order fit of the same data. Sigmaplot allows the user to fit implicit fuctions by nonlinear regression. Since the function with A subtracted on both sides is still in the domain of absorbance, the comparison with first-order is straightforward.

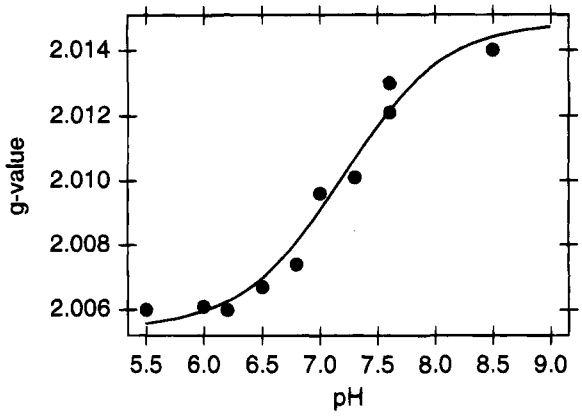

FIGURE 2: pH dependence of the EPR spectrum of center C. The g value of the $g \sim 2.01$ resonance was measured as a function of pH. The line is from a fit to eq 8 and defines limiting g values as 2.0054 ± 0.0004 (low pH) and 2.0149 ± 0.0006 (high pH) and the pK_a as 7.2 ± 0.1.

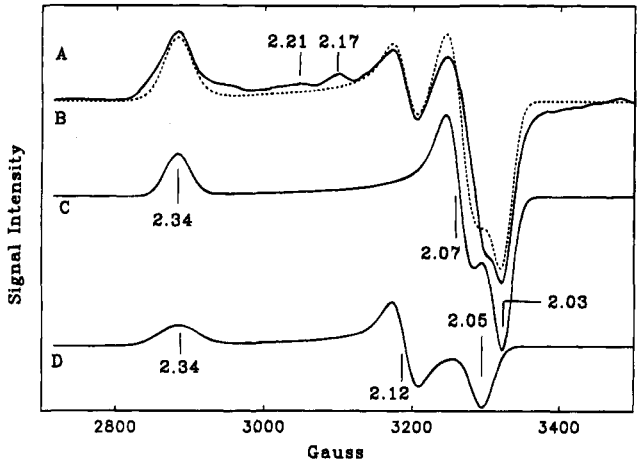

FIGURE 3: Simulation of EPR spectrum from the CODH–thiocyanate adduct. The spectrum was simulated using the program XPOW (Belford & Nilges, 1979; Nilges, 1979; Altman, 1981; Maurice, 1982; Duliba, 1983). (A) EPR spectrum of CODH–thiocyanate adduct, conditions as in Figure 1B, except the frequency was 9.4408 GHz. (B) (- - -) Simulated EPR spectrum of the CODH–thiocyanate adduct including 80% component I (g_{av} = 2.15) and 20% component II (g_{av} = 2.17). (C) Spectral simulation of isolated component I. The g values and full linewidths at half-height (in MHz) were 2.34 (65), 2.067 (50), and 2.03 (42). (D) Spectral simulation of isolated component II: 2.34 (100), 2.115 (50), and 2.047 (50).

and Fe are components of center C (Qiu *et al.*, 1995), the EPR spectrum of the thiocyanate adduct reveals a small degree of hyperfine broadening (~6 G) from ^{57}Fe (Figure 1D) and not from ^{61}Ni substitution (Figure 1C).

Simulation of the EPR spectrum of the anion-treated enzyme required two components: one with $g_{av} = 2.15$ and another one with $g_{av} = 2.17$ in a 80:20 ratio (Figure 3). Minor features at $g = 2.21$ and 2.17 could not be included in the simulation of the two-component spectrum. The maximum intensity of the EPR signal was 0.3 spins per mol of α,β dimer. The EPR spectrum after reaction of CODH with sodium azide or sodium cyanate was indistinguishable from that of the thiocyanate adduct. This is not due to a general salt effect. Addition of sodium chloride did not elicit the profound changes in the EPR spectrum observed with thiocyanate, cyanate, or azide.

Reduction of the thiocyanate-treated enzyme with dithionite or CO caused disappearance of the $g_{av} = 2.15$ and 2.17 signals and appearance of the EPR spectra of the low

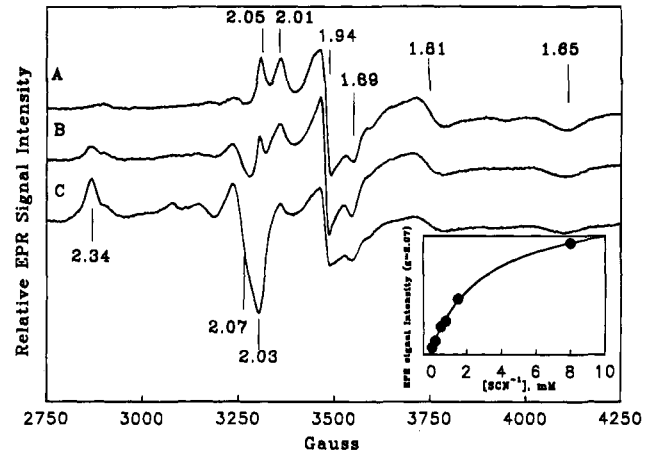

FIGURE 4: EPR titration of binding of thiocyanate to CODH. (A) CODH (50 μM, final) mixed with 0.2 mM thiocyanate, under conditions as for Figure 1B. (B) 2 mM thiocyanate. (C) 8 mM thiocyanate. (Inset) The intensity of the resonance at $g = 2.07$ was plotted as a function of thiocyanate concentration and fit to eq 9 yielding a K_d of 3.2 mM.

potential form of center C (called center C′) (g = 1.97, 1.86, 1.75) (Kumar *et al.*, 1993) and of center B (g = 2.04, 1.94, 1.89). When the thiocyanate incubated enzyme was treated with CO (but not with dithionite), the Ni–Fe–C EPR signal was observed. When thiocyanate was added to samples of CODH that had been incubated with the mild reductant dithiothreitol, to a state where the EPR signals from both centers B and C were present, the spectrum of center B was unchanged, but that of center C was replaced with the g_{av} = 2.15 signal characteristic of the thiocyanate adduct.

The g_{av} = 2.15 EPR signal broadened above 30 K, and the $P_{1/2}$ at 10 K was greater than 400 mW. These properties are like those of the EPR signal from unligated center C, which also is fast relaxing and difficult to saturate with microwave power (Lindahl *et al.*, 1990a,b). These properties are atypical for iron-sulfur clusters.

The intensity of this signal increased and that of the unligated form of center C decreased as the concentration of thiocyanate was increased. Analysis of the intensity of the g_{av} = 2.15 EPR signal as a function of thiocyanate concentration yielded a dissociation constant (K_d) at pH 7.6 of 3.2 ± 0.3 mM (Figure 4). Analysis of the signal intensity as a function of azide concentration yielded a K_d of 12.8 ± 1.8 mM.

Thiocyanate and azide also influenced the electronic spectrum of CODH (Figure 5). When thiocyanate or azide was reacted with CODH, an increase in absorbance at 440 nm and a decrease at 350 nm was observed. These concentration-dependent absorption changes were plotted versus the concentration of anion and analyzed by eq 9,

$$A = (A_{max}[\text{Anion}])/(K_d + [\text{Anion}]) \quad (9)$$

where A and A_{max} represent the observed and maximal difference absorption changes, respectively. The $\Delta\epsilon$ at 440 nm was 754 M^{-1} cm^{-1}. The value of K_d was found to be 9.1 ± 0.6 for thiocyanate (Figure 5) and 12.8 ± 1.8 mM for azide (data not shown). These values are similar to those obtained by EPR spectroscopic titrations.

pH and Temperature Dependence of CO Oxidation. Our results indicate that CO oxidation follows a ping-pong mechanism. Initial velocity data at pH 7.6 and 25 °C (inset, Figure 6) are consistent with a ping-pong mechanism. A

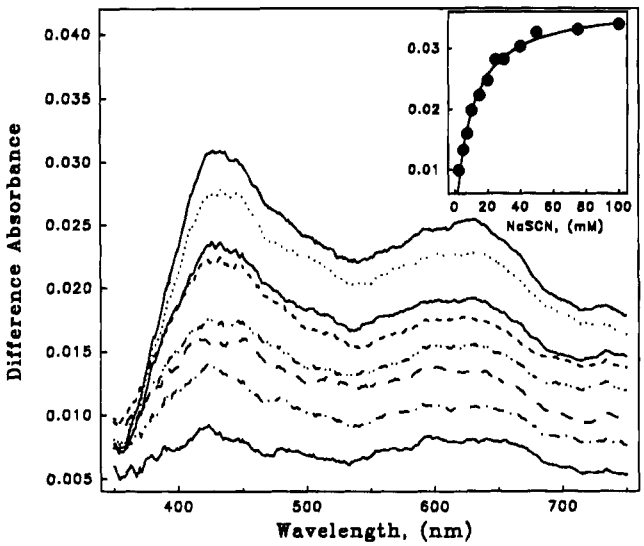

FIGURE 5: Binding of sodium thiocyanate to CODH. UV−visible spectra were recorded of 32.2 μM CODH (final) in 50 mM Tris-HCl, pH 7.6, and 2 mM DTT at various concentrations of sodium thiocyanate. The sodium thiocyanate was added from a 5 M stock prepared in the same buffer. The spectrum of CODH was subtracted from that of CODH in thiocyanate, smoothed by the adjacent data averaging (10 points) routine (Microcal Origin), and graphed by Sigma Plot. The difference spectra shown are of CODH incubated with 2.5, 5, 7.5, 10, 15, 20, 30, and 40 mM thiocyanate. (Inset) The absorption maximum at 440 nm was plotted as a function of thiocyanate concentration and data were fit to eq 9 to yield a K_d of 9.1 ± 0.6 mM.

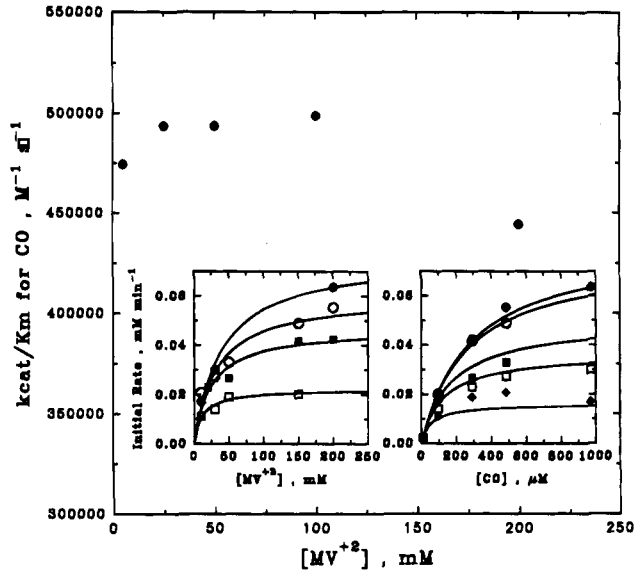

FIGURE 6: Dependence of V/K for CO on the concentration of methyl viologen. The reaction was performed at 25 °C in buffer containing 133 mM Tris-HCl, pH 7.4, 2 mM DTT, 10% (9.7 μM) CO, 90% N_2, and varying concentrations of methyl viologen. The CODH concentration was 45 nM ($\alpha\beta$ dimers). Values of V/K for CO were obtained by fitting the absorbance increase at 604 nm to the equation $A = A_o + (A_i - A_o)[1 - \exp(-tV/K)]$. (Insets) Initial velocity studies of CO oxidation. (Left inset) Dependence of the initial rate on CO concentration at the following methyl viologen concentrations: 200 mM (●), 150 mM (○), 50 mM (■), 30 mM (□), and 10 mM (◆). Other conditions are 25 °C, 100 mM Tris-HCl, pH 7.50, and 9 nM CODH ($\alpha\beta$ dimers). (Right inset) Replot of the same data versus the methyl viologen concentration at the following CO concentrations: 970 μM (●), 480 μM (○), 290 μM (■), and 97 μM (□). The curves are fits to a ping-pong mechanism with k_{cat} = 190 ± 20 s^{-1}, K_m (CO) = 360 ± 70 μM, and K_m (MV) = 55 ± 9 mM.

ping-pong mechanism for CO oxidation was also proposed in earlier studies with cell extracts from *C. thermoaceticum* (Diekert & Thauer, 1978) and *C. pasteurianum* (Thauer *et al.*, 1974). A stringent method for distinguishing ping-pong from ternary-complex mechanisms is to measure k_{cat}/K_m for one substrate with an excess of the second substrate. In ping-pong mechanisms, the k_{cat}/K_m for one substrate is independent of the concentration of the other substrate. The k_{cat}/K_m for CO did not increase over a 50-fold range in concentration of methyl viologen (Figure 6). There was a slight decrease in k_{cat}/K_m for CO at high concentrations of methyl viologen (5% decrease at 200 mM), presumably due to substrate inhibition. These combined results are in accord with a ping-pong mechanism and inconsistent with a ternary complex mechanism.

The kinetic parameters obtained by initial velocity kinetics (Figure 6) were the same as those measured under similar conditions with the integrated Michaelis−Menten equation (below), justifying use of the integrated equation for further mechanistic studies of CO oxidation. The CO oxidation reaction was studied at 25 °C and at pH values between pH 5.5 and 10.8. Both k_{cat} and k_{cat}/K_m were found to be pH dependent (Figure 7 and Table 1). The data were fit to eqs 3 and 4, yielding the parameters given in Table 2. For k_{cat}/K_m, a single titration was observed with a pK_a of 7.7 ± 0.2, reaching a plateau with a maximum value of 9 × 10^5 M^{-1} s^{-1} at 25 °C. At pH 7.6 and 55 °C, the k_{cat}/K_m was 4.2 × 10^6 M^{-1} s^{-1}; therefore, assuming that the pH profiles at 55 and 25 °C are identical, the maximum value of k_{cat}/K_m at 55 °C can be calculated to be 9.1 × 10^6 M^{-1} s^{-1}. Two distinct titration curves were observed for k_{cat}, with pK_a values of 7.0 and 9.5. At pH 7.6 and 55 °C, the value of k_{cat} was 600 s^{-1}. An unsatisfactory fit to a single titration curve is shown in dotted lines. According to the pH profile, the extrapolated maximum value of k_{cat} at 55 °C is 3250 s^{-1}, equivalent to a specific activity of 1310 μmol min^{-1} mg^{-1}.

The pK_a values obtained here are in qualitative agreement with earlier studies of the CO oxidation reaction catalyzed by the CODH from *C. pasteurianum* (Thauer *et al.*, 1974). In this case, the initial velocity increased as the pH increased with an inflection point at pH 8.5.

The temperature dependencies of k_{cat} and k_{cat}/K_m were studied (Figure 8A). Fitting these data to the Eyring equation gave values for $\Delta H^{\ddagger}$ of 53.2 kJ mol^{-1} and $\Delta S^{\ddagger}$ of 44.2 J mol^{-1} K^{-1} for k_{cat}/K_m (with a standard state for CO of 1 M). The calculated values for k_{cat} were 55.7 kJ mol^{-1} and −22.4 J mol^{-1} K^{-1}. The maximum values of k_{cat} and k_{cat}/K_m (at 55 °C and high pH) calculated from the Eyring equation were similar to the values calculated from the pH dependence data (given above).

The K_d values for thiocyanate (3−10 mM) and azide (13 mM) were obtained by titrations that were monitored by EPR and UV−visible spectroscopy. The K_{is} value at pH 7.6 was 36 ± 20 mM. The K_{is} value is higher; however, given the standard error for the measurement, it coincides with the K_d measurements.

Inhibition of CO Oxidation and CO_2 Reduction by Thiocyanate. Thiocyanate was found to inhibit CO oxidation and CO_2 reduction. It can be classed as a mixed inhibitor with respect to CO in the CO oxidation reaction because the values of K_{is} and K_{ii} were significantly different. The notations for K_{is} and K_{ii} were described by Cleland (1970). As shown in Figure 9, thiocyanate was a partial mixed inhibitor with respect to CO.

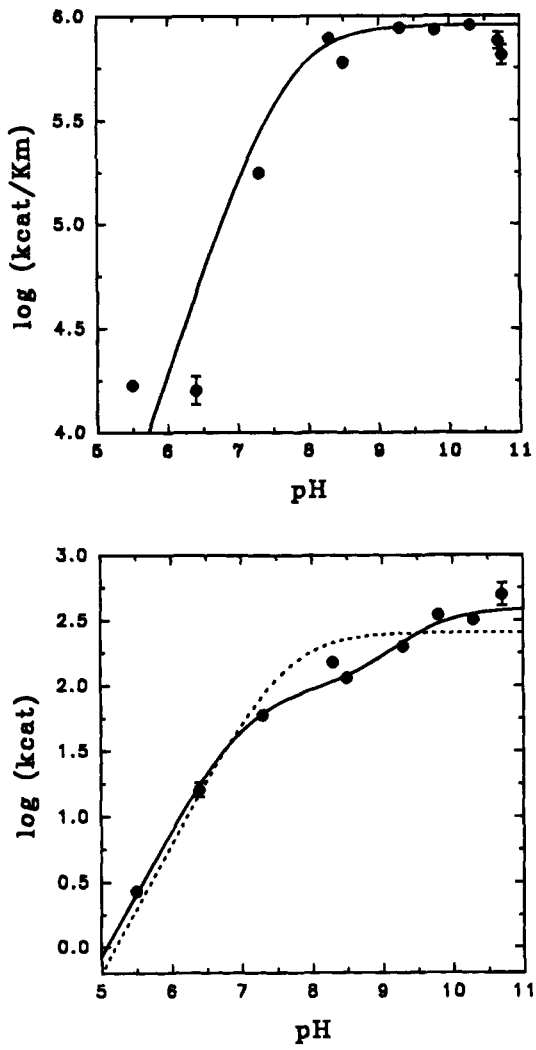

FIGURE 7: pH profile of $\log(k_{cat}/K_m)$ and $\log(k_{cat})$ for CO oxidation. Fits correspond to eqs 3 and 4, the data are given in Table 1, and the kinetic parameters are shown in Table 2. Conditions were 25 °C, 90 or 100% CO, 10 mM methyl viologen, and either 50 or 100 mM buffer, λ = 504 nm, cell path = 2 mm. The k_{cat}/K_m and k_{cat} values were the same at 50 or 100 mM buffer concentration. The fit parameters for the single titration (dotted line) are $(kk_{cat})_{max}$= 255 ± 50 s^{-1} and pK_{ai} = 7.60 ± 0.2.

Partial mixed inhibition was observed at almost all pH values and temperatures. Although when K_{ii} was very large (>1 M), we did not observe the plateau, since this would have required concentrations of thiocyanate greater than 4 M.[2]

Thiocyanate was found to be a much stronger inhibitor at low pH values. Both K_{is} and K_{ii} were found to be pH dependent (Table 1 and Figure 10). The inhibition data were fit to eqs 10 and 11 where K_1 and K_3 are the inhibition

$$K_{is} = K_1 + K_2\left(\frac{K_{as}}{K_{as} + [H^+]}\right) \quad (10)$$

$$K_{ii} = K_3 + K_4\left(\frac{K_{ai}}{K_{ai} + [H^+]}\right) \quad (11)$$

constants of thiocyanate for the species represented by k_{cat}/K_m and k_{cat} at limiting low pH; K_2 and K_4 are the corresponding inhibition constants at limiting high pH. Thus, the values of K_{is} and K_{ii} both were found to plateau at low and high pH values and gave pK_a values of ~7.7 (Table 2).

Inhibition by thiocyanate of the reverse reaction, i.e., reduction of CO_2 to CO, was also studied. Thiocyanate was found to be a mixed inhibitor with respect to CO_2. The value of K_{is} for CO_2 reduction was equivalent to the value of K_{ii} for CO oxidation (Table 1). The assay relies on the rapid and irreversible binding of hemoglobin to CO and could be performed in the presence of the inhibitor thiocyanate.[3]

The thermodynamics of thiocyanate binding to CODH were determined by measuring the dependence of K_{ii} and K_{is} on temperature. Van't Hoff plots of the ln K_{ii} versus $1/T$ and the ln K_{is} versus $1/T$ are shown in Figure 8B. The inhibition data were fit to eq 12 to give the enthalpic (ΔH)

$$-nRT \ln K_i = \Delta G_d^\circ = \Delta H_d - T\delta S_d \quad (12)$$

and entropic (ΔS) contributions to the dissociation of thiocyanate, where n is the number of sites (assumed to be unity), R is the gas constant, and ΔG_d, ΔH_d, and ΔS_d represent the free energy, enthalpy, and entropy changes upon thiocyanate dissociation. This study yielded values of ΔH = 41 ± 5 kJ mol^{-1} and ΔS = 170 ± 20 J K^{-1} mol^{-1} for K_{is}. For K_{ii}, the values were ΔH = 26 ± 10 kJ mol^{-1} and ΔS = 120 ± 30 J K^{-1} mol^{-1}. The extrapolated values of K_{is} and K_{ii} at 0 °C and pH 7.6 were 6.3 ± 0.8 and 20 ± 10 mM, respectively.

Although dissociation of thiocyanate is disfavored by a positive enthalpic term, it is favored by an offsetting increase in entropy yielding a free energy of dissociation from oxidized center C of −10 kJ mol^{-1} at 25 °C and −15 kJ mol^{-1} at 55 °C. Therefore, there is a sufficiently large decrease in entropy to slightly disfavor the binding of thiocyanate to center C. We observed a linear dependence of ln K_{ii} and ln K_{is} on $1/T$ over the 50 °C temperature range studied, suggesting that the enthalpy value is independent of temperature and that binding of thiocyanate to CODH occurs without a change in heat capacity.

DISCUSSION

The ability to interconvert CO and CO_2 is essential for anaerobic organisms to grow autrotrophically using the Wood/Ljungdahl pathway. This capability also is required for anaerobes to convert acetic acid to methane or to oxidize acetic acid during sulfate reduction. This reaction is catalyzed by center C, which appears to be the second Ni/Fe-S cluster identified in the CODH from *C. thermoaceticum* (Qiu *et al.*, 1995). In the work described here, we have focused on the mechanism of CO oxidation and inhibition of this reaction by anions. Previously, cyanide was shown to act as a potent slow-binding inhibitor of this reaction (Ragsdale *et al.*, 1983a; Ensign *et al.*, 1989b; Morton, 1991; Anderson & Lindahl, 1994) and to bind to center C (Anderson *et al.*, 1993a). Here, we have focused on a class

[2] The effects of these anions are not general salt effects. With sodium chloride, there is about a 12% decrease in *V*/K as the concentration is increased from 0 to 200 mM. We observed a 20% increase in *V*/K between 400 and 1000 mM. As described above, there is no change in the EPR properties of the enzyme in the presence of 500 mM sodium chloride.

[3] In control experiments, we demonstrated that thiocyanate did not perturb the detection of CO. When aliquots of CO-saturated buffer were added to a solution of reduced hemoglobin, the spectra associated with formation of the hemoglobin−CO adduct were identical whether thiocyanate was present or absent. In addition, whether thiocyanate was present or absent, the traces of absorbance versus time were linear during the period of time where initial rates were monitored (5 min).

Table 1: pH Dependence of CO Oxidation Parameters and Inhibition Constants for Thiocyanate

pH	log (k_{cat}/K_m) (M^{-1} s^{-1})	K_{is} (mM)	log k_{cat} (s^{-1})	K_{ii} (mM)
5.50	4.22 ± 0.02	16 ± 5	0.43 ± 0.02	30 ± 10
6.40	4.20 ± 0.07	12.5 ± 0.9	1.20 ± 0.05	102 ± 10
7.30	5.25 ± 0.01	160 ± 40	1.778 ± 0.007	320 ± 20
8.30	5.89 ± 0.02	190 ± 80[a]	2.18 ± 0.03	2200 ± 750
8.50	5.78 ± 0.02	520 ± 110	2.061 ± 0.004	1130 ± 60
9.30	5.942 ± 0.004	750 ± 30	2.30 ± 0.04	970 ± 440
9.80	5.93 ± 0.02	570 ± 130	2.54 ± 0.02	
10.30	5.96 ± 0.01	620 ± 60	2.51 ± 0.01	1320 ± 100
10.75	5.81 ± 0.05	790 ± 310[a]	3.03 ± 0.02	720 ± 270
10.70	6.20 ± 0.02	520 ± 120	2.70 ± 0.09	
10.70	5.88 ± 0.04	830 ± 250	2.89 ± 0.03	
6.0 (CO_2 reduction)[b]	2.2 ± 0.2	140 ± 40	−1.75 ± 0.10	700 ± 200

[a] Data for k_{cat}/K_m at these pH values were fitted with offset. [b] K_{is} and K_{ii} were determined as described in text.

Table 2: Parameters for the pH Dependence of CO Oxidation and Thiocyanate Inhibition

	parameters for k_{cat}/K_m	parameters for k_{cat}
pH-profile parameters		
maximal rate 1	$(k_{cat}/K_m)_{max}$ = (9.0 ± 1.2) × 10^5 M^{-1} s^{-1}	k_{cat1} = 90 ± 20 s^{-1}
pK_{a_1}	pK_{as} = 7.7 ± 0.7	pK_{ai1} = 7.05 ± 0.13
maximal rate 2		k_{cat2} = 300 ± 60 s^{-1}
pK_{a_2}		pK_{ai2} = 9.46 ± 0.32
NaSCN inhibition parameters		
low-pH K_i (mM)	K_1 = 6 ± 14	K_3 = 50 ± 60
pK_a	7.8 ± 1.0	7.6 ± 0.7
high-pH K_i (mM)	K_2 = 700 ± 60	K_4 = 1200 ± 200

of anions that are rapid binding inhibitors and elicit large changes in the EPR spectra of center C.

The EPR spectrum of CODH is markedly altered when thiocyanate, azide, or cyanate bind. Several results indicate that the spectra are from the reversible and specific formation of an adduct between the anion and center C. (i) When CODH is incubated with anions, the EPR spectrum of center C decreases as the g_{av} = 2.15−2.17 signals increase. (ii) The relaxation properties (temperature and power dependence of the EPR signals) of the anion adducts are similar to those of center C and are very different from those of center A or B. (iii) The K_d values measured by EPR and UV−visible spectroscopic titrations are similar to the inhibition constant for the free enzyme−thiocyanate complex determined by steady-state kinetic experiments.[4] (iv) The pH dependence of the EPR spectrum of center C matches those of CO oxidation and thiocyanate inhibition of this reaction. (v) Electron spin echo envelope modulation studies using $^{14}N_3$ and $^{15}N_3$ demonstrate that azide nitrogens are directly coordinated to the center that gives rise to the 2.15 and 2.17 EPR signals (Kumar *et al.*, 1995). It is surprising that anions that are noncompetitive inhibitors with relatively high K_i values have more marked effects on the EPR spectrum of center C than does cyanide which is a potent competitive inhibitor.

Besides altering the EPR signal for center C, thiocyanate was found to be a pH-dependent mixed inhibitor with respect to CO. Inhibition by thiocyanate was found to be partial; i.e., at saturation with the inhibitor, the rate does not drop to zero (Figure 2). Incomplete inhibition could arise from

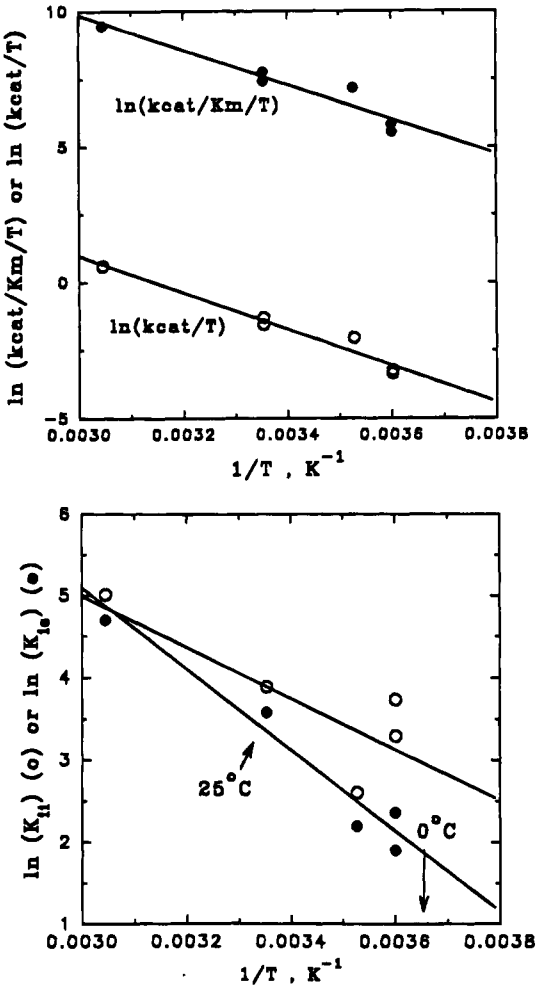

FIGURE 8: Temperature dependence of CO oxidation and its inhibition by thiocyanate. (A, top) The reaction was performed at 25 °C in a solution containing 10 mM methyl viologen, 90% CO, and 50 mM Tris-HCl buffer, pH 7.60. Values of V/K and V were obtained using eq 2. Fitting to the Eyring eq 12 gave values for $\Delta H^{\ddagger}$ of 53.2 kJ mol^{-1} and $\Delta S^{\ddagger}$ of 44.2 J mol^{-1} K^{-1} for k_{cat}/K_m. (B, bottom) The values of K_{is} and K_{ii} were obtained according to eqs 5 and 6. Nonlinear regression analysis to a van't Hoff plot yielded values of ΔH = 41 ± 5 kJ mol^{-1} and ΔS = 170 ± 20 J K^{-1} mol^{-1} for K_{is} and values of ΔH = 26 ± 10 kJ mol^{-1} and ΔS = 120 ± 30 J K^{-1} mol^{-1} for K_{ii}. The extrapolated values of K_{is} and K_{ii} at 273.15 K are 6.3 ± 0.8 and 20 ± 10 mM, respectively.

(a) thiocyanate acting as an alternate substrate, (b) thiocyanate binding at another metal center in CODH (center A or B), (c) center C existing in two (or more) heterogeneous forms, all able to perform CO oxidation but (at least) one unable to bind thiocyanate, and (d) the inhibitor interacting at a site on center C where neither CO or water bind.

[4] The K_d values for thiocyanate (3−10 mM) and azide (13 mM) were obtained by titrations monitored by EPR and UV−visible spectroscopy. The K_{is} value at pH 7.6 was 36 ± 20 mM. The K_{is} value is higher; however, given the standard error for the measurement, it coincides with the K_d measurements.

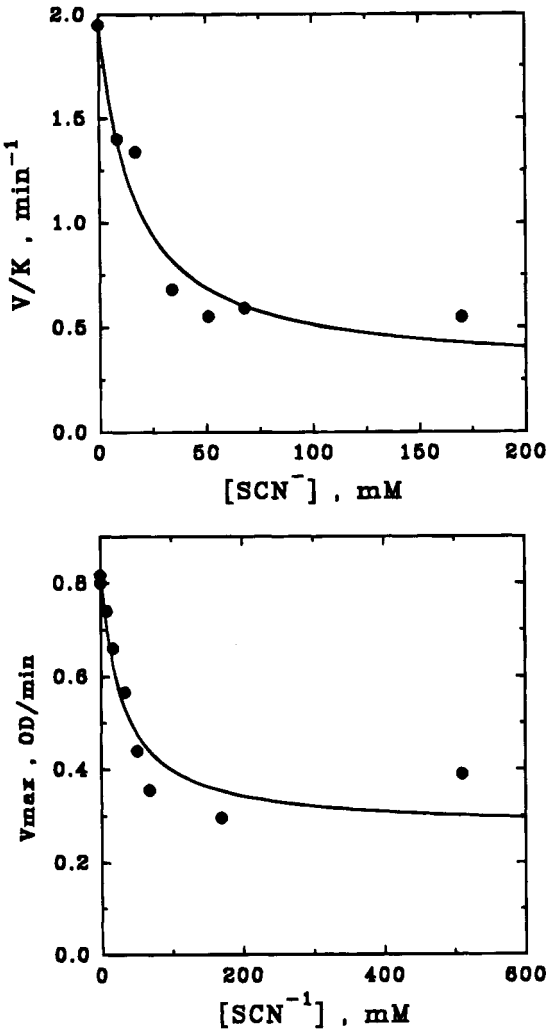

FIGURE 9: Inhibition of CO oxidation by thiocyanate at pH 5.50. The curves are fits to eqs 5 and 6 with $(V/K)_o = 1.97 \pm 0.12$ min^{-1}, K_{is}=16 ± 5 mM, and $(V/K)_{in} = 0.28 \pm 0.11$ min^{-1} for V/K and $(k_{cat})_o = 0.82 \pm 0.04$ OD min^{-1}, $K_{ii} = 30 \pm 12$ mM, $(k_{cat})_{in} = 0.27 \pm 0.06$ OD min^{-1}. Other conditions are 10 mM methyl viologen, 1.94 μM CODH, 25 °C, 100% CO, λ = 504 nm, and cell path = 2 mm.

Thiocyanate does not appear to be an alternate substrate since (i) CODH does not reduce methyl viologen with thiocyanate as electron donor (data not shown) and (ii) since partial inhibition is observed for both k_{cat} and k_{cat}/K_m, both oxidized and reduced forms of CODH must react with thiocyanate. Explanation (b) is unlikely since our results indicated that thiocyanate binds *only* to center C. Explanation (c) that invokes heterogeneity of center C is appealing because (i) the EPR signals for center C in the free and anion-treated forms account for 0.3 instead of 1.0 spins per $\alpha\beta$-dimer and (ii) there are at least two EPR spectra associated with the anion adduct. Explanation (d) cannot be ruled out and predicts that reaction of thiocyanate-treated CODH with CO or dithionite would reduce the enzyme. This could substantially increase the K_d for thiocyanate, which would be reflected in the EPR spectrum of the reduced form of center C.

In order to develop a scheme to explain the mechanism of inhibition, it was necessary to better characterize the mechanism of CO oxidation. Previous (Thauer *et al.*, 1974; Diekert & Thauer, 1978) steady-state studies along with those reported here indicate that this reaction occurs by a ping-pong mechanism; i.e., CO_2 release precedes binding of the

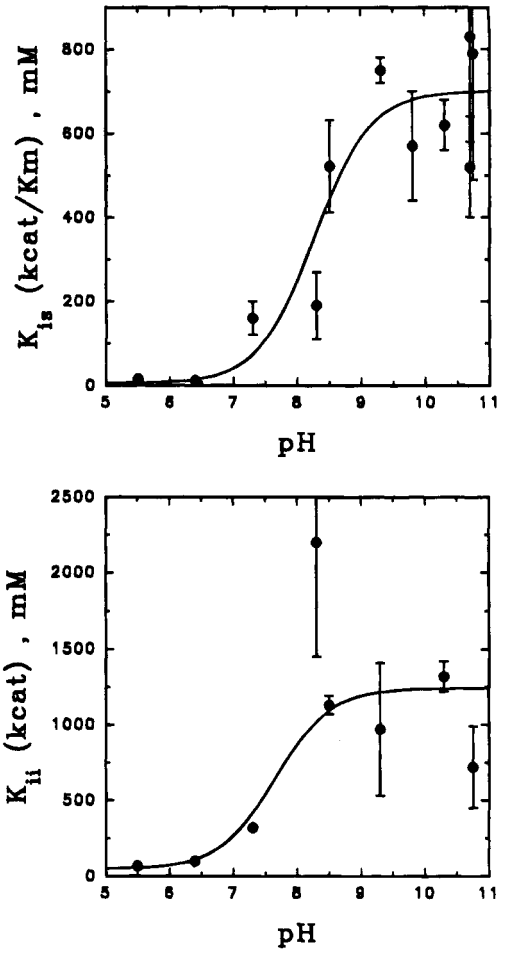

FIGURE 10: Inhibition of CO oxidation by thiocyanate. The values of K_{is} and K_{ii} from Table 1 were plotted versus pH and fit to eqs 10 and 11. The calculated parameters from the fit are shown in Table 2. Other conditions are described in the caption of Figure 8 and under Materials and Methods.

Scheme 1

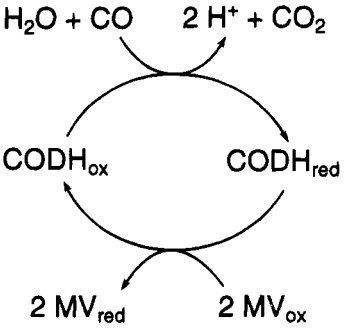

oxidant as shown by Scheme 1. This is consistent with the results of a pre-steady-state study that characterized the steps involved in the first half-reaction of CO oxidation (Kumar *et al.*, 1993).

Schemes 2 and 3 expand the first half-reaction of the ping-pong mechanism shown in Scheme 1. These schemes offer different explanations for the pH dependences of k_{cat}/K_m and k_{cat}. They also account for the pH dependence of thiocyanate inhibition including four states to which thiocyanate could bind. This is necessary since a single titration for K_{is} with limiting values at low (K_1) and high (K_2) pH and a single titration for K_{ii} with limiting values at low (K_3) and high (K_4) pH were observed.

Deprotonation of enzyme-bound carboxyl could give rise to a pH-dependent k_{cat}. However, this ionization is unlikely

Scheme 2

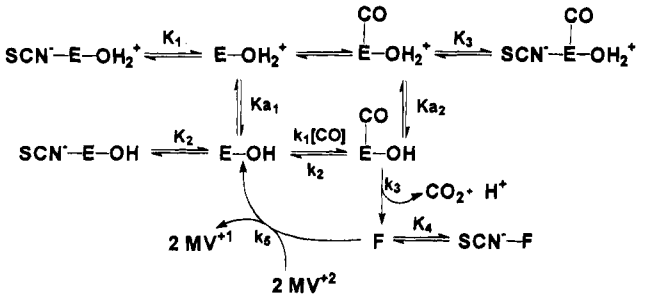

Scheme 3

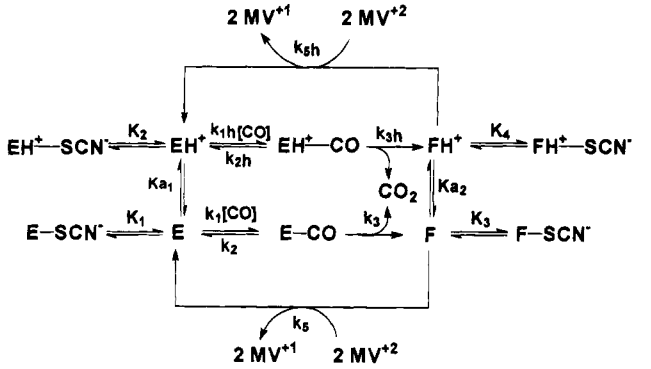

to be responsible for any of the observed pK_a values since the pK_a value for a free carboxyl is ~4 and that for a metal-bound carboxyl would be expected to be even lower.

In Scheme 2, the pH dependence of k_{cat}/K_m for CO oxidation (pK_a = 7.2) is assumed to originate in the deprotonation of enzyme-bound water in its binary complex with center C. The pH dependence of the EPR spectrum of center C would reflect the same ionization event. At low pH, the enzyme would be inactive because enzyme-bound hydroxide is required for catalysis. The observed pK_a is not inconsistent with that of water coordinated to the Ni or one of the Fe sites in center C. Water bound to divalent metal complexes can have pK_a values as low as 7 (Bertini & Luchinat, 1994), and coordinated water in carbonic anhydrase has a pK_a of 6 (Silverman & Lindskog, 1988). The pH dependence of k_{cat} is assumed to derive from deprotonation of water in the ternary complex between center C, water, and CO. Thus, binding of CO would slightly decrease the pK_a for enzyme-bound water.

According to Scheme 2, the pH dependences of K_{is} and K_{ii} are defined by eqs 13 and 14, where K_{a_1} and K_{a_2} would

$$K_{is} = \frac{(K_{a_1} + 10^{-pH})K_2}{\frac{K_2 K_{a_1}}{K_1} + 10^{-pH}} \quad (13)$$

$$K_{ii} = \frac{(K_{a_2} + 10^{-pH})K_4}{\frac{K_4 K_{a_2}}{K_3} + 10^{-pH}} \quad (14)$$

reflect the ionization constants for water in the E–OH_2 and E–$CO(OH_2)$ complexes. Consistent with this mechanism, we observe four species to which thiocyanate can bind corresponding to K_1–K_4. Also consistent with this interpretation, the pK_{a_1} and pK_{a_2} (~7.5) are similar to the pK_a values determined from measuring the pH dependences of k_{cat}/K_m and k_{cat}. The pH dependence of K_{is} would originate from differential affinity of thiocyanate for the aquo- and hydroxo-forms of center C. The pH dependence of K_{ii} would result from the different affinity of thiocyanate for the inactive E–CO–OH_2 complex at high pH and to "F" at low pH.

An alternative explanation for the pH dependence of CO oxidation and of inhibition by thiocyanate is presented in Scheme 3. For simplicity, the complex between water (or hydroxide) and the enzyme is ignored. Scheme 3 summarizes the general class of mechanisms in which the pH dependence of k_{cat}/K_m originates from ionization of an amino acid residue in the free enzyme. This residue would act as a base presumably to remove a proton from bound H_2O to yield the active nucleophilic E–OH^- species. In Scheme 3, the pH-dependent change in the EPR spectra could derive from an indirect effect of alteration of the ionic environment near center C as the active site base undergoes ionization. In this type of mechanism, the k_{cat}/K_m and k_{cat} for the CO oxidation reaction must plateau at high and low pH values. Our data are inconsistent with this prediction because both k_{cat}/K_m and k_{cat} show a single titration with no detectable rate below pH 5.5. This indicates that the species FH^+, if it exists, does not turn over and is not kinetically relevant.

Scheme 3 also includes the class of mechanisms that interpret the thiocyanate inhibition data as reflecting different binding affinities of thiocyanate for the "protonated" and "unprotonated" forms of $CODH_{ox}$ (designated as E and EH^+) and $CODH_{red}$ (designated as F and FH^+). The pH dependence of the inhibition constants K_{is} and K_{ii} should reflect ionization of the same active-site base that determines the pH dependence of V/K and V. Observation of four species (corresponding to K_1–K_4) to which thiocyanate can bind is consistent with this mechanism. However, an inconsistency between Scheme 3 and our results is that the K_{ii} for CO oxidation with thiocyanate at pH 6.0 (30–120 mM) is very similar to K_{is} for CO_2 reduction (140 mM). This indicates that both inhibition constants may reflect the binding of thiocyanate to $CODH_{red}$ (designated as F), which is consistent with Scheme 2, but inconsistent with Scheme 3.

For the reasons described above, we favor the mechanism described in Scheme 2. However, it is difficult to unambiguously confirm or reject either mechanism. Studies directed at characterization of the metal–oxygen bond of the bound water or hydroxyl species, determination of the pK_a of such a species, identification of the metal, and evaluation of the mechanism of proton transfer will be required for such a judgement.

There is a large enough decrease in entropy to make binding of thiocyanate mildly unfavorable thermodynamically. Thus, one observes stronger inhibition at low temperatures. The lack of a heat-capacity change associated with binding or dissociation of thiocyanate is characteristic of electrostatic and hydrogen bonding interactions (DeLauder *et al.*, 1994). Thus, it appears that binding of thiocyanate to center C results in stronger, more ordered, and possibly electrostatically stabilized interactions at the Ni/Fe-S cluster. If this network of interactions between thiocyanate and center C interferes with the binding of CO or water, the inhibitory role of anions at the active site could be rationalized. This interpretation would be consistent with noncompetitive nature of inhibition of thiocyanate with respect to both CO and water. The situation could be similar to the binding of cyanide to cytochrome *c* peroxidase. In this case, a decrease

in entropy has been found to accompany binding of cyanide which results in a network of hydrogen bonds and rearrangement of water molecules at the active site (DeLauder *et al.*, 1994).

The mechanism of CO oxidation could be related to that of carbonic anhydrase that binds water and CO_2 and uses metal-bound hydroxide as a nucleophile. In this case, one observes a pH dependence only on k_{cat} and not on k_{cat}/K_m since transfer of the proton from enzyme-bound water to buffer is fully rate limiting (Silverman & Lindskog, 1988). The mechanism also could be similar to that of other iron–sulfur hydrolytic enzymes like aconitase, where one of the irons in the [4Fe-4S] cluster binds the substrates, *cis*-aconitate and hydroxide (Werst *et al.*, 1990; Kilpatrick *et al.*, 1994).

REFERENCES

Altman, T. E. (1981) Analysis of Nuclear Quadrupole Coupling in EPR Spectra, Ph.D. dissertation, University of Illinois at Urbana-Champaign.

Anderson, M. E., & Lindahl, P. A. (1994) *Biochemistry 33*, 8702–8711.

Anderson, M. E., DeRose, V. J., Hoffman, B. M., & Lindahl, P. A. (1993a) *J. Am. Chem. Soc. 115*, 12204–12205.

Anderson, M. E., DeRose, V. J., Hoffman, B. M., & Lindahl, P. A. (1993b) *J. Inorg. Biochem. 51*, Abstract B149.

Andreesen, J. R., Schaupp, A., Neurater, C., Brown, A., & Ljungdahl, L. G. (1973) *J. Bacteriol. 114*, 743–751.

Aresta, M., Quaranta, E., & Tommasi, I. (1988) *J. Chem. Soc. Chem. Commun.*, 450–452.

Begley, M., Collin, J.-P., Ruppert, R., & Sauvage, J.-P. (1986) *J. Am. Chem. Soc. 108*, 7461–7467.

Belford, R. L., & Nilges, M. J. (1979) in *EPR Symposium*, 21st Rocky Mountain Conference, Denver, CO.

Bertini, I., & Luchinat, C. (1994) in *Bioinorganic Chemistry* (Bertini, I., Gray, H. B., Lippard, S. J., & Valentine, J. S., Eds.) pp 37–106, University Science Books, Mill Valley, CA.

Bonam, D., & Ludden, P. W. (1987) *J. Biol. Chem. 262*, 2980–2987.

Bott, M., & Thauer, R. K. (1989) *Z. Naturforsch. 44*, 392–396.

Budavari, S., Ed. (1989) in *The Merck Index*, 11 ed., Merck & Co., Rahway, NJ.

Cleland, W. W. (1970) in *The Enzymes* (Boyer, P., Ed.) Vol. 2, Academic Press, New York.

DeLauder, S. F., Mauro, J. M., Poulos, T. L., Williams, J. C., & Schwarz, F. P. (1994) *Biochem. J. 302*, 437–442.

Diekert, G. B., & Thauer, R. K. (1978) *J. Bacteriol. 136*, 597–606.

Duliba, E. P. (1983) Studies of Nuclear Quadrupole Effects in Transition Metal Complexes by Electron Paramagnetic Resonance, Ph.D. dissertation University of Illinois at Urbana-Champaign.

Elliott, J. I., & Brewer, J. M. (1978) *Arch. Biochem. Biophys. 190*, 351–357.

Ensign, S. A., Bonam, D., & Ludden, P. W. (1989a) *Biochemistry 28*, 4968.

Ensign, S. A., Hyman, M. R., & Ludden, P. W. (1989b) *Biochemistry 28*, 4973–4979.

Fan, C., Gorst, C. M., Ragsdale, S. W., & Hoffman, B. M. (1991) *Biochemistry 30*, 431–435.

Ferry, J. G. (1992a) *Crit. Rev. Biochem. Mol. Biol. 27*, 473–502.

Ferry, J. G. (1992b) *J. Bacteriol. 174*, 5489–5495.

Fuchs, G. (1986) *FEMS Microbiol. Rev. 39*, 181–213.

Gorst, C. M., & Ragsdale, S. W. (1991) *J. Biol. Chem. 266*, 20687–20693.

Harder, S. A., Feinberg, B. F., & Ragsdale, S. W. (1989a) *Anal. Biochem. 181*, 283–287.

Harder, S. A., Lu, W.-P., Feinberg, B. F., & Ragsdale, S. W. (1989b) *Biochemistry 28*, 9080–9087.

Kilpatrick, L., Kennedy, M. C., Beinert, H., Czernuszewicz, R. S., Qiu, D., & Spiro, T. G. (1994) *J. Am. Chem. Soc. 116*, 4053–4061.

Kumar, M., & Ragsdale, S. W. (1992) *J. Am. Chem. Soc. 114*, 8713–8715.

Kumar, M., Lu, W.-P., Liu, L., & Ragsdale, S. W. (1993) *J. Am. Chem. Soc. 115*, 11646–11647.

Kumar, M., Lu, W.-P., & Ragsdale, S. W. (1994) *Biochemistry 33*, 9769–9777.

Kumar, M., Lu, W.-P., Smith, A., Ragsdale, S. W., & McCracken, J. (1995) *J. Am. Chem. Soc. 117*, 2939–2940.

Lindahl, P. A., Münck, E., & Ragsdale, S. W. (1990a) *J. Biol. Chem. 265*, 3873–3879.

Lindahl, P. A., Ragsdale, S. W., & Münck, E. (1990b) *J. Biol. Chem. 265*, 3880–3888.

Ljungdahl, L. G. (1986) *Annu. Rev. Microbiol. 40*, 415–450.

Lu, Z., White, C., Rheingold, A. L., & Crabtree, R. H. (1993) *Angew. Chem., Int. Ed. Engl. 32*, 92–94.

Maurice, A. M. (1982) Acquisition of Anisotropic Information, Ph.D. dissertation University of Illinois at Urbana-Champaign.

Morton, T. A. (1991) Sequencing and Active Site Studies of Carbon Monoxide Dehydrogenase/Acetyl-CoA Synthase from *Clostridium thermoaceticum*, Ph.D. dissertation University of Georgia.

Nilges, M. J. (1979) Electron Paramagnetic Resonance Studies of Low Symmetry Nickel I and Molybdenum V Complexes, Ph.D. dissertation University of Illinois at Urbana-Champaign.

Qiu, D., Kumar, M., Ragsdale, S. W., & Spiro, T. G. (1994) *Science 264*, 817–819.

Qiu, D., Kumar, M., Ragsdale, S. W., & Spiro, T. G. (1995) *J. Am. Chem. Soc. 117*, 2653–2654.

Ragsdale, S. W. (1991) *CRC Crit. Rev. Biochem. Mol. Biol. 26*, 261–300.

Ragsdale, S. W. (1994) in *Acetogenesis* (Drake, H. L., Ed.) pp 88–129, Chapman and Hall, New York.

Ragsdale, S. W., & Wood, H. G. (1985) *J. Biol. Chem. 260*, 3970–3977.

Ragsdale, S. W., Ljungdahl, L. G., & DerVartanian, D. V. (1982) *Biochem. Biophys. Res. Commun. 108*, 658–663.

Ragsdale, S. W., Clark, J. E., Ljungdahl, L. G., Lundie, L. L., & Drake, H. L. (1983a) *J. Biol. Chem. 258*, 2364–2369.

Ragsdale, S. W., Ljungdahl, L. G., & DerVartanian, D. V. (1983b) *Biochem. Biophys. Res. Commun. 115*, 658–665.

Ragsdale, S. W., Wood, H. G., & Antholine, W. E. (1985) *Proc. Natl. Acad. Sci. U.S.A. 82*, 6811–6814.

Raybuck, S. A., Bastian, N. R., Orne-Johnson, W. H., & Walsh, C. T. (1988) *Biochemistry 27*, 7698–7702.

Rupp, H., Rao, K. K., Hall, D. O., & Cammack, R. (1978) *Biochim. Biophys. Acta 537*, 255–269.

Segel, I. H. (1975) in *Enzyme Kinetics*, John Wiley & Sons, San Francisco.

Shin, W., & Lindahl, P. A. (1992) *Biochemistry 31*, 12870–12875.

Shin, W., Stafford, P. R., & Lindahl, P. A. (1992) *Biochemistry 31*, 6003–6011.

Silverman, D. N., & Lindskog, S. (1988) *Acc. Chem. Res. 21*, 30–36.

Stephens, P. J., McKenna, M.-C., Ensign, S. A., Bonam, D., & Ludden, P. W. (1989) *J. Biol. Chem. 264*, 16347–16350.

Tan, G. O., Ensign, S. A., Ciurli, S., Scott, M. J., Hedman, B., Holm, R. H., Ludden, P. W., Korszun, Z. R., Stephens, P. J., & Hodgson, K. O. (1992) *Proc. Natl. Acad. Sci. U.S.A. 89*, 4427–4431.

Thauer, R. K., Fuchs, G., Käufer, B., & Schnitker, U. (1974) *Eur. J. Biochem. 45*, 343–349.

Thauer, R. K., Möller-Zinkhan, D., & Spormann, A. M. (1989) *Annu. Rev. Microbiol. 43*, 43–67.

Werst, M. M., Kennedy, M. C., Beinert, H., & Hoffman, B. (1990) *Biochemistry 29*, 10526–10532.

BI950010Q